Article

Feasibility Study on the Potential Replacement of Primary Raw Materials in Traditional Ceramics by Clayey Overburden Sterile from the Prosilio Region (Western Macedonia, Greece)

Angeliki Christogerou [1,2,*] **, Paraskevi Lampropoulou** [3] **, Dimitrios Papoulis** [3] **and George N. Angelopoulos** [1,2]

[1] Department of Chemical Engineering, University of Patras, Caratheodori 1, 26504 Patras, Greece; angel@upatras.gr

[2] INVALOR: Research Infrastructure for Waste Valorization and Sustainable Management, Caratheodory 1, University Campus, 26504 Patras, Greece

[3] Geology Department, University of Patras, 26504 Patras, Greece; p.lampropoulou@upatras.gr (P.L.); papoulis@upatras.gr (D.P.)

[*] Correspondence: angiechristo@upatras.gr

Abstract: The objective of this study was to investigate the valorization potential of clayey overburden sterile materials from lignite-mining activities in the manufacturing of traditional ceramics. This study aims to contribute toward the sustainable management and use of such waste materials in line with the environmental objectives of the 2030 agenda. To assess this issue, clayey steriles were incorporated in a white clay-body at 20, 50, and 80 wt%, whereas reference samples were also formed from the individual raw materials. Laboratory processing of the ceramics was performed by dry pressing loose powder into rectangular samples and firing at 1000 °C for 4 h. Characterization of the raw materials included chemical, mineralogical, and thermal analysis. The fired bodies were tested for their total linear shrinkage, apparent porosity, water absorption, bulk density, and bending strength according to the relevant standards. The microstructural evolution of the final bodies was analyzed by scanning electron microscopy, which observed differences related to the addition of the steriles. The results showed that the tested clayey steriles can be utilized up to 50 wt% as a secondary raw material in the production of ceramic materials (e.g., bricks) with comparable properties to the reference clay-bodies. Furthermore, the color of the final samples changed from white-creamy to reddish as the content of clayey sterile materials increased in the raw mix.

Keywords: smectite clayey steriles; valorization; secondary raw materials; clay-based ceramics; technological properties; pigment

1. Introduction

Nowadays, the modern way of life and human demands are strongly related to different natural resources (e.g., metallic and non-metallic minerals, fossil fuels, and biomass) and their applications in a wide range of fields. Their uses have tripled since 1970, in accordance with mining excavations and/or drilling exploitations [1]. The mining activities alone produce a large amount of wastes, exceeding 100 billion tones/year, and they are responsible for about 50% of global greenhouse gas emissions [1,2]. These wastes include different materials, such as tailings, waste rocks (steriles), and slags, which all require appropriate treatment and management under the frame of environmental and economic sustainability [3]. Many previous investigations have presented different environmental pollution problems, health risks, and other negative effects on the societies, communities, and economies derived from mining such waste deposits [4,5]. In recent years, industries obeying ethical implications (e.g., Mine Waste Directive, 2006/21/EC [6]) and/or other international official environmental agreements (e.g., Paris agreement (COP21) [7], "European Green Deal" [8]) have invested in improved mining technologies and the development of waste treatment processes, hence facing an increasing total management

cost [9–11]. Therefore, cheap alternatives are being sought. In this direction, research activities related to the valorization and/or remediation of mining wastes have increased and are focused on the conservation of natural raw materials under the prism of circular economy principles [10–14].

Industrial production strategies, as well as regional and/or national policies, are required to develop the management of the available resources. A sound example is the significant volume of wastes and residues which are produced today due to industrialization. In this context, we should point out that we consider the above materials, the wastes and residues, as potential natural resources [15]. On the other hand, the above policies and strategies should be able to "decouple" economic growth from the utilization of natural resources. Therefore, the utilization of secondary raw materials, such as wastes and residues, are at the forefront of this effort.

In the case of the ceramic industry, its broad market continues to grow, with an annual rate of ~8.5% [16]. In particular, for the extraction of non-metallic minerals (clay deposits included), their global extraction rate accounts for 48%; 4.9 times higher in 2017 than in 1970 [17]. Besides this, the wastes that arise from mining activities are increasing accordingly. In the EU, mining and quarrying wastes accounted for more than 25% in 2018 of all wastes generated by economic and household activities [18].

Clays are the most common raw materials used for ceramic production, especially in the field of traditional ceramics. Globally, there is a wide range of clay-based raw materials used for different ceramic applications, such as mullite-based refractory materials, bricks and tiles, porcelain, stoneware, etc. [19–21] Previous investigations have demonstrated that there are different mining steriles or other wastes with similar compositions and comparable properties appropriate for new competitive (even improved and energy-efficient) ceramic products, compared to the commercial ones [11,22]. Over the last decade, there has been an increasing scientific interest in the use of alternative raw materials in ceramics derived from mining wastes (e.g., iron mining wastes, boron mining wastes, kaolin steriles, granite steriles, coal mining steriles), aiming for the sustainability and symbiosis of industries in conjunction with environmental protection. However, investigations on the utilization of mining wastes for the production of energy-efficient ceramic materials should be carried out more intensively in the future. Industry stakeholders would be less susceptible to adapting such alternative raw materials in industrial established processes [11,12,23–26].

Coal mining activities represent a high percentage of global material extraction combined with high amounts of different kinds of wastes. Among these wastes, previous investigations related to the utilization of sterile clayey rocks in different fields of application, including ceramic materials, have been conducted [26,27].

The objective of this study was to evaluate the valorization potential of clayey sterile materials (CSM) from the Prosilio Region in Greece as secondary raw materials for the formation of bricks and/or roofing tiles. So far, to the best of our knowledge, no similar work has been officially published with this specific type of sterile, which motivated the authors to conduct this first-approach investigation. Finally, the viable end-use of these steriles may be an alternative solution to the disposed volumes in the respective area.

2. Materials and Methods

2.1. Materials

The study area belongs to the NW part of the Hellenic mountain chain where, since the Miocene, the crust extended to form a complex pattern of basins [28]. These basins accumulated up to 600 m thick during the late Miocene and late Pliocene age sequence. This sequence includes a basal conglomerate–sandstone unit followed by lacustrine–fluvial sand-clays grading upward into lignite horizons [29]. The clayey sterile samples used for this study were located close to the upper part of the sediments accumulated in the so-called Servia lignite-bearing basin. In particular, the clayey samples were derived from the open-pit mine in the Prosilio region, Kozani (western Macedonia, Greece, Figure 1).

In total, the sterile samples are on average 6–10 m in thickness. The Prosilio open-pit covers a 2,263,198 m² area. The borders of the Servia basin comprise Pelagonian terrain rocks, primarily composed of Paleozoic schists, Carboniferous granites, and Mesozoic limestones [30]. Clay sediments overlay lignite deposits in depths of approximately 40–120 m and are characterized mainly as xylite. The clayey sterile samples used in this study represent a high-smectite content material (Figure 1). Though, it should be noted that other horizons with lower-smectite content also exist in this open-pit mine. However, the reference clay material, which is replaced by CSM, is a calcium-rich clay-body (W) from the northwestern Peloponnese (Greece), commercially used for the manufacturing of white-creamy roofing tiles and supplied from a local ceramic industry.

Figure 1. Top view of the open-pit mine in Prosilio region (Kozani, NW Greece) with indicative sampling points (white arrows) of the studied clayey steriles.

2.2. Formation of Ceramic Samples

The raw materials were dried at 110 °C for 24 h and milled in a planetary mill to a particle size <125 μm. Three blends were prepared, consisting of W and CSM in different proportions. Specifically, CSM was added at 20, 50, and 80 wt%, replacing the respective amount of the clay-body (W). Thereafter, the produced samples were named as W20, W50, and W80. Reference samples consisting of 100 wt% W and CSM, respectively, were also formed for comparison with the blended ones. Homogenization of the dry powders was carried out in a plastic bag that was hermetically sealed and thoroughly stirred for about 10 min. Afterwards, water was added by spraying in order to ensure a minimum moisture content of 6–8 wt%, necessary for the shaping method of dry pressing [31]. Compaction of the rectangular samples (100 mm × 20 mm × 10 mm) was achieved by filling loose materials in a stainless-steel mold and applying uniaxial pressure at about 225 bar using a hydraulic piston pump (ENERPAC, XA12G, 720 W JAMES ST, Columbus, WI, USA). The green bodies were left overnight at room temperature and, afterwards, in a laboratory oven for drying at 110 °C until they were constant in weight. Firing took place with a controlled temperature gradient in an electrical muffle furnace up to 1000 °C following a 36 h thermal cycle including heating and cooling to room temperature. The soaking time at the peak temperature lasted 4 h.

2.3. Characterization of Raw Materials and Ceramics

For both raw materials, several analyses were performed in order to determine their physico-chemical and thermal properties. Powder X-ray diffraction (XRD) analysis was applied for the detection of mineralogical phases using a Bruker D8 Advance Diffractometer (Bruker, Billerica, MA, USA) with CuKα radiation at 40 kV and 30 mA. The 2θ scanning range was between 2 and 70° for bulk composition samples, and 2 and 20° for clay fractions (prepared after air drying and treatment with ethylene glycol). The step size was 0.015°/0.1 s. For the qualitative identification of the mineralogical phases, DIFFRACplus EVA v.12® software (Bruker-AXS, Billerica, MA, USA) was used, based on the ICDD Powder Diffraction File of PDF-2 2006. The semi-quantitative analyses of bulk compositions were based on the peak area method and calculated using the same software (EVA®) and its "Area tool". The chemical composition was determined with a RIGAKU ZSX PRIMUS II wavelength dispersive spectrometer (WD-XRF) equipped with a 4 KW Rh X-ray tube using pressed pellets. Simultaneous thermal analysis measurements were conducted by means of Differential Scanning Calorimetry and Thermogravimetry (DSC/TG) using the NETZSCH STA 449*F3* Jupiter® (NETZSCH-Gerätebau GmbH, Selb, Germany) which runs under the Proteus® software (Version 5.2.1/29 November 2011). Powder samples taken from the humidified blends (Section 2.2) were placed in alumina crucibles with a pierced lid and heated over a controlled temperature ramp at 10 °K/min from 25 to 1000 °C under a nitrogen atmosphere.

The ceramic samples were evaluated for their physico-mechanical properties according to relevant standard methods and techniques. Total linear shrinkage after firing was determined according to ASTM C 326 [32]. Apparent porosity, water absorption, and bulk density were measured following the procedures of the ASTM C 373 [33] standard. Investigation of the developed microstructures was carried out by SEM (JSM-6300, Jeol, Tokyo, Japan) on gold-coated ceramic surfaces. Flexural strength was evaluated using the DILLON testing machine (model: DTM, Force Measurement Products and Systems, Fairmont, MN, USA) equipped with a three-point bend attachment. A constant rate of 1 mm/min was applied for the load displacement until failure of the ceramic beams occurred.

3. Results and Discussion

3.1. Physico-Chemical Properties of Raw Materials

#### 3.1.1. Chemical and Mineralogical Composition

The results of the X-ray fluorescence (XRF) analysis are shown in Table 1. The reference clay-body presents a typical chemical composition of a Ca-rich clay suitable for the manufacturing of white-creamy ceramic products (e.g., bricks and/or roofing tiles). The clayey sterile materials consist mainly of SiO_2, Al_2O_3, Fe_2O_3, and MgO along with minor components, such as CaO, K_2O, TiO_2, and Na_2O. The main differences among the two raw materials are in the content of alkaline earth oxides (CaO and MgO), which for W is about 15.8% and, for CSM, ~5.9%. These are known as important sintering promoters in the production of ceramic materials. Additionally, the fluxing oxides (Na_2O and K_2O) are higher in the case of W (~3.1%), as in CSM (~1.1%). The higher amount of Fe_2O_3 in CSM is noteworthy, at about double that of W (5.3%), which anticipates the formation of the enhanced liquid phase during firing, but also changes related to the final color of the samples.

Regarding the mineralogical composition (Figure 2), the clay-body consists of quartz, albite, calcite, and phyllosilicate minerals of chlorite and illite/muscovite. As for the studied clayey sterile, differences are observed in the received XRD-pattern compared to the reference clay-body. It is characterized as bentonite clay since it consists mainly of smectite (84 wt%) and lower amounts of quartz (6 wt%), calcite (5 wt%), alkali feldspars (2 wt%), and other phyllosilicates (3 wt%).

Table 1. Chemical composition (in wt%) of the raw materials W and CSM and their blends W20, W50, and W80 (calculated).

	SiO_2	Al_2O_3	CaO	Fe_2O_3	MgO	K_2O	Na_2O	TiO_2	L.O.I
W	48.29	13.61	12.72	5.30	3.11	2.49	0.59	bdl	13.64
W20	48.91	14.10	10.42	6.24	3.40	2.19	0.51	0.21	13.42
W50	49.82	14.84	7.01	7.64	3.84	1.73	0.36	0.51	13.15
W80	50.73	15.59	3.60	9.04	4.29	1.26	0.22	0.81	12.88
CSM	51.34	16.09	1.32	9.98	4.58	0.95	0.13	1.03	12.70

bdl = below detection limits.
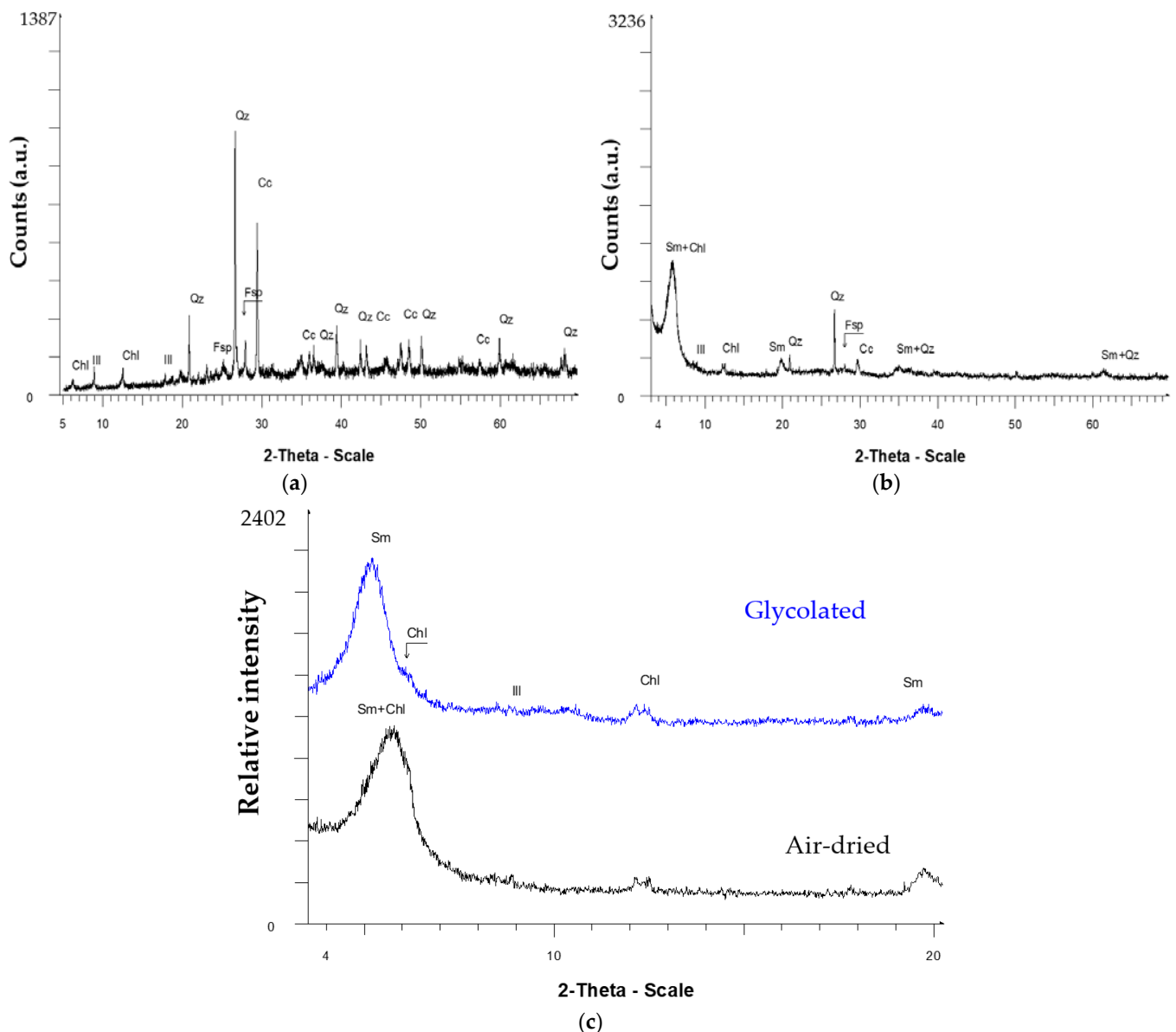
Figure 2. Powder X-ray diffraction patterns of the (**a**) clay-body (W), (**b**) clayey overburden sterile (CSM), and (**c**) clay fraction of CS. Abbreviations: Cc—calcite; Chl—chlorite; Fsp—feldspar; Ill—illite; Sm—smectite, Qz—quartz.

3.1.2. Thermal Analysis

A simultaneous TG-DSC analysis was applied to investigate the firing behavior of the individual raw materials and their mixtures, the results of which are depicted in Figure 3. The clay-body was also used in other experimental studies [34] and presents a typical

behavior of a Ca-rich clay-body over the studied temperature range (25–1000 °C), with a total mass loss of about 13.4%, mainly attributed to calcite decomposition occurring between 700 and 810 °C. The CSM sample shows minor variations in dehydration behavior, with distinct differences in the endothermic peak system (DSC curve) compared to W, mainly due to the different mineralogical composition. Thus, for heating up to 150 °C, a strong endothermic peak is observed resulting from dehydration reactions of sorbed moisture, mostly interlayered, typical for smectite group minerals. During this decomposition, a gradual continuous mass loss of about 18.7% is evident on the respective TG curve (Figure 3a). This content falls within the humidity range (7.9–18.9%) stated elsewhere [23] for a similar clayey sterile. In the temperature region of 450–550 °C, a small endothermic deflection appears with a maximum at 500 °C, ascribed to the dehydroxylation phenomena, with a corresponding mass loss of 6.7%, approximately. In some instances, the dehydroxylation of smectite minerals may also be observed in other temperature intervals than the above described, and this mainly depends on their mineral sub-groups, i.e., dioctahedral and trioctahedral, which are characterized by different cation-exchange capacities [35]. Generally, throughout the phyllosilicates, the dehydroxylation peak of magnesium species always appears at higher temperatures (e.g., 770–860 °C), whereas for Fe-smectites, it appears at lower temperatures (e.g., 450–520 °C) [36,37]. The latter is also observed in the case of the studied CSM. With the further increase in temperature, a broad endo-peak in the 600–850 °C region can be distinguished, with a maximum at 750 °C, followed by a small exo-peak at about 900 °C, associated with structural rearrangements upon dehydroxylation and recrystallization to new phases. For the three blends, W20, W50, and W80, similar TG-DSC curves are obtained but with markable displacements of the endo-peak in the 680–800 °C region (Figure 3b). The differences may vary up to 80 °C with respect to the maximum peak of the reference clay-body (795 °C). Certainly, this behavior may be related to the CSM content in the raw mix, as for W20, W50, and W80, this peak is given at 762 °C, 745 °C, and 713 °C, respectively. In conjunction with this, the mass losses (Figure 3a) show no further reduction after heating at 800 °C, indicating that all decomposition reactions are completed at this point. Seemingly, sintering of the ceramic bodies may also be achieved at 50 °C lower than 1000 °C, as indicated from the DSC results and the peak representing crystallization on new phases at about 900 °C. Nevertheless, this assumption needs to be further investigated by testing the additional firing temperatures of the green samples (e.g., 900 and 950 °C).

3.2. Final Properties of Ceramic Samples

3.2.1. Mineralogical Composition

The mineralogical phases detected after firing at 1000 °C are presented in Figure 4. In the case of the reference sample W, it consists mainly of primary quartz and the new phases of Ca-feldspars (anorthite), and less sanidine, as well as low amounts of diopside, gehlenite, and hematite formed after the decomposition of phyllosilicate minerals and calcite contained in the raw material. Despite the similar mineralogy, the W20 sample presents lower quartz intensities and higher ones in the case of feldspars, diopside, and hematite compared to W. This is attributed mainly to the decomposition upon the firing of the clay minerals included in CSM. Besides, higher concentrations of fluxing agents such as iron oxide further enhance the reaction kinetics. Generally, it is noticed from the XRD patterns that the increase in clayey steriles in the reference clay-body (W) leads to a reduction in quartz intensities. Nevertheless, in the sample with 50 wt% of clayey sterile (W50), diopside or gehlenite are distinguished with difficulty due to the lower calcium oxide concentrations, while alkali feldspars seem to predominate. Moreover, hematite peak intensity indicates an increase while spinel group minerals were detected (mainly as solid solution of hercynite and spinel). The W80 sample consists of lower quartz and feldspars compared to W50 and higher amounts of hematite and spinels, while the polymorph of SiO_2 cristobalite is clearly detected. Due to the high transformation and high expansion of cristobalite associated with volume decrease upon cooling, ceramic bodies may suffer

from this inversion if no sufficient flux is available to produce an adequate glassy phase in which it can dissolve. This polymorph of silica (cristobalite) presents a volume change during inversion which is greater than that of quartz. Regarding the fired clayey sterile sample (CSM), it indicates a more amorphous character with lower peak intensities of quartz and other crystalline phases (mainly spinel, hematite, and cristobalite). This mineral composition demonstrates that during firing, the decomposition of predominant smectite led to a fine amorphous homogeneous matrix, while the crystallization was not favored at 1000 °C, despite the higher amounts of liquid phases.
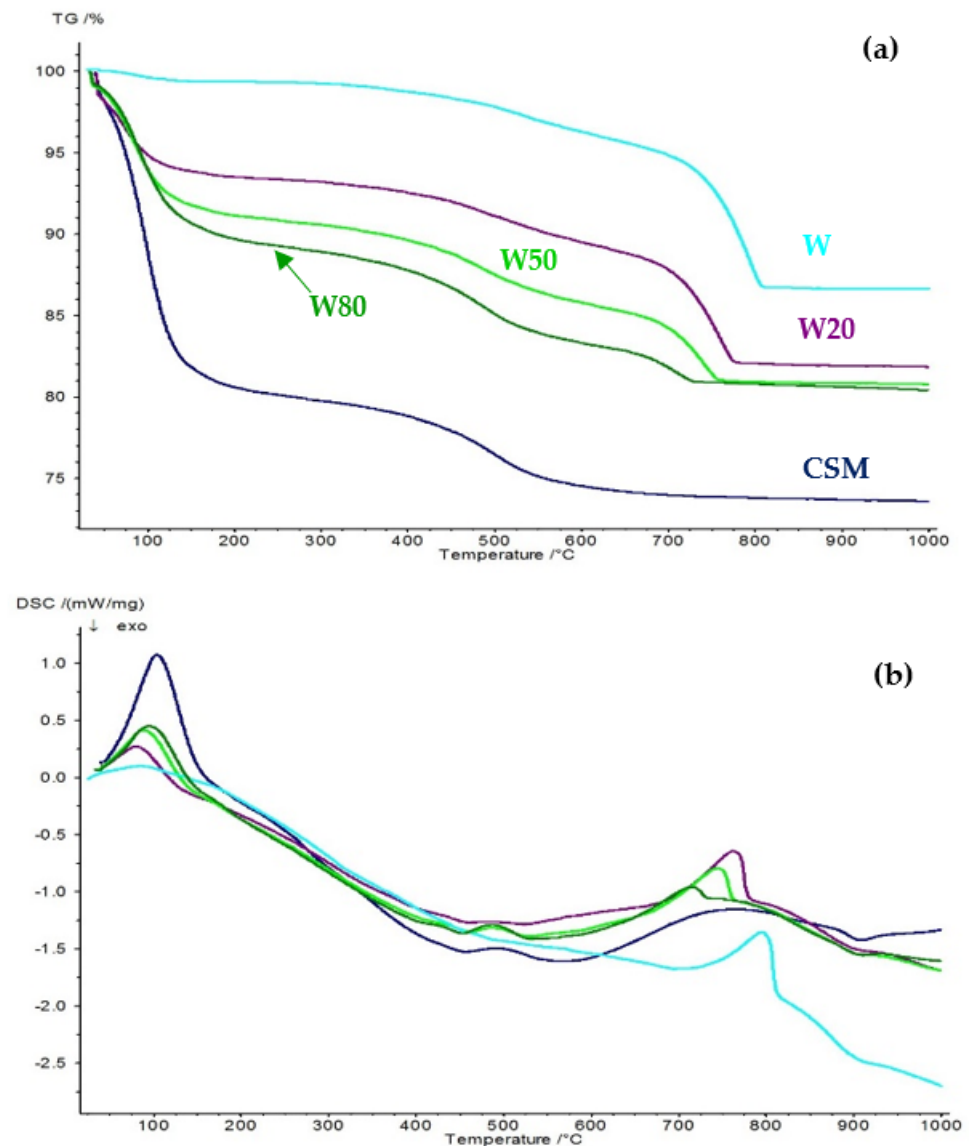

Figure 3. (**a**) TG and (**b**) DSC curves of the raw materials (W and CSM) and their blends (W20, W50, W80). Heating rate 10 K/min under nitrogen atmosphere.
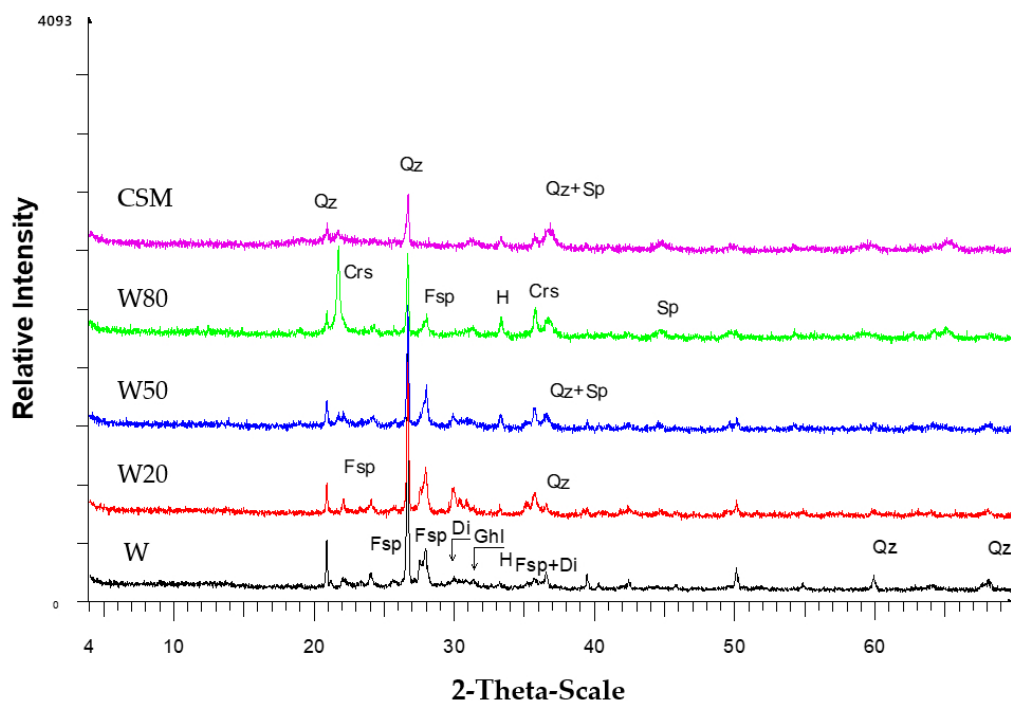
Figure 4. Powder X-ray diffraction patterns of the fired samples at 1000 °C. Abbreviations: Qz—quartz, Crs—cristobalite, Sp—spinel, Fsp—feldspar, Di—diopside, Ghl—gehlenite, H—hematite.

3.2.2. Physico-Mechanical Properties

The results of the physical and mechanical properties determined on fired samples are shown in Table 2. It is obvious that the quality of the end products is clearly affected by the addition of CSM in the reference clay-body. In particular, the increase in CSM content leads to dimensional changes in the samples, as presented by the increased values of total linear shrinkage after firing (LS), which is more evident for substitutions over 50 wt%. Accordingly, a compact structure seems to have been formed during firing, as reflected by the decreased apparent porosity (AP) and the increased bulk density (BD) values with respect to the reference body. In the case of flexural strength, the samples W20 and W50 present values of about 23 MPa, close to the bending strength obtained for W (24.5 MPa). However, a strong decrease of about 47% is observed for samples W80 in comparison to the reference ones, but still within the specifications of clay bricks (>5 MPa). Ceramics consisting of 100 wt% CSM present a variety of small cracks on their surface after firing (Figure 5), mainly attributed to the higher linear shrinkage (11.95%) in comparison with the other samples. This phenomenon is associated with phase transition and the crystallization of new phases (~900 °C), which is in total agreement with the respective endo/exo effects observed by the DSC analysis (Figure 3). Consequently, mechanical testing on representative samples was not possible. However, only one individual sample that did not present visible defects on its surface underwent bending failure and yielded a value of about 6 MPa. An important parameter affecting the mechanical durability may be the brittleness of smectite-rich clay-bodies, which is associated with their higher shrinking–swelling capacity than other clay minerals [38]. Cracking phenomena and dimensional stability problems of the fired sample may also arise if, within the increased amount of the amorphous phase, no appropriate fillers are present (e.g., quartz) in order to stabilize the final structure (Figure 4).

Table 2. Technological properties of fired samples. LS: linear shrinkage after firing, AP: apparent porosity, WA: water absorption, BD: bulk density and 3PBS: three-point bending strength.

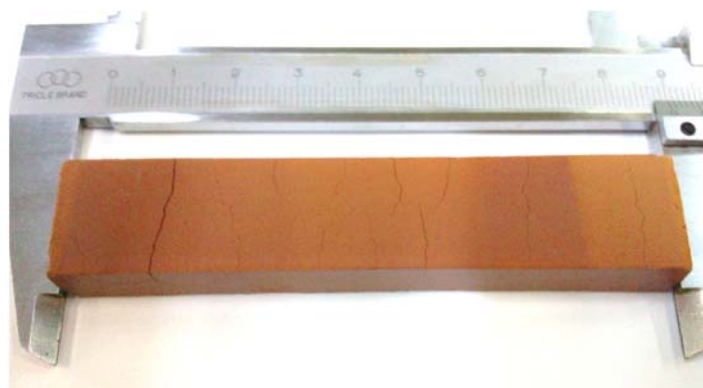|	LS (%)	AP (%)	WA (%)	BD (g/cm^3)	3PBS (MPa)
W	1.45 ± 0.06	31.65 ± 0.66	16.9 ± 0.4	1.87 ± 0.01	24.52 ± 1.71
W20	1.95 ± 0.11	30.11 ± 0.43	16.4 ± 0.3	1.84 ± 0.01	23.11 ± 2.16
W50	3.14 ± 0.06	27.34 ± 0.25	14.3 ± 0.2	1.91 ± 0.01	23.02 ± 3.23
W80	8.19 ± 0.06	15.75 ± 0.50	7.3 ± 0.3	2.16 ± 0.01	12.91 ± 2.83
CSM	11.95 ± 0.15	11.60 ± 1.03	5.0 ± 0.5	2.34 ± 0.03	nd

nd = not determined.

Figure 5. Fired sample consisting only of CSM (100 wt%). Visible cracks appear on the surface.

Moreover, the phase transitions during firing clearly affected the color appearance of the final specimens, as shown in Figure 6. The increase in CSM in the clay-body gradually changed the hue of the ceramics from creamy-ochre to reddish. Additionally, the sample with 100% of CSM presented an intensified red-orange color, mainly due to higher amounts of iron-bearing phases.
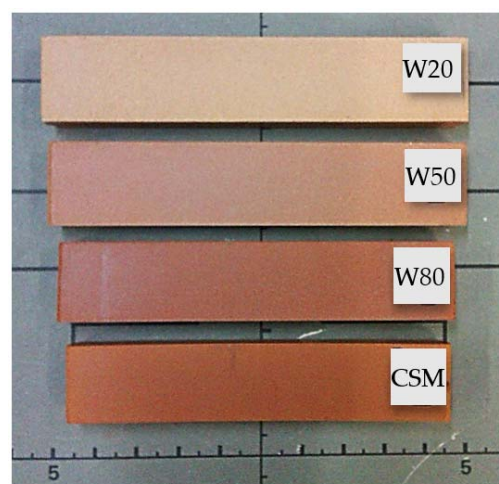

Figure 6. Ceramics' hue variation in relation to CSM content. Transition from ochre-white to reddish color with increase in CSM.

3.2.3. Microstructural Evolution

Figure 7 shows secondary electron images of polished ceramic surfaces. The reference sample (Figure 7a) shows a typical microstructure of a ceramic body, characterized by open and interconnected porosity where quartz grains can be distinguished. With the addition of the clayey sterile into to the clay-body, alterations are observed in the morphology of the

ceramic matrix denoted by the different appearance of crystal grains (e.g., their smaller size) and the irregular development of porosity, mainly in the case of W20 (Figure 7b). For W50 (Figure 7c), however, a decrease in porosity is observed, along with an increase in vitrified regions, where quartz grains have been dissolved in agreement with the reduced peak intensity of quartz, as indicated by XRD results (Figure 4). The ceramic sample with the highest substitution amount of CSM (W80) consists predominantly of the amorphous phase, resulting in a denser microstructure than the previous tested blends (W20 and W50) in accordance with the higher bulk density and the increased linear shrinkage after firing, as depicted in Table 2. This evolution of microstructure is more pronounced in the case of the CSM sample (Figure 7d), where porosity is almost diminished due to the enhanced liquid phase formation. No grains are visible in this micrograph, indicating that all clay minerals underwent complete transformation or were completely dissolved in the liquid phase.
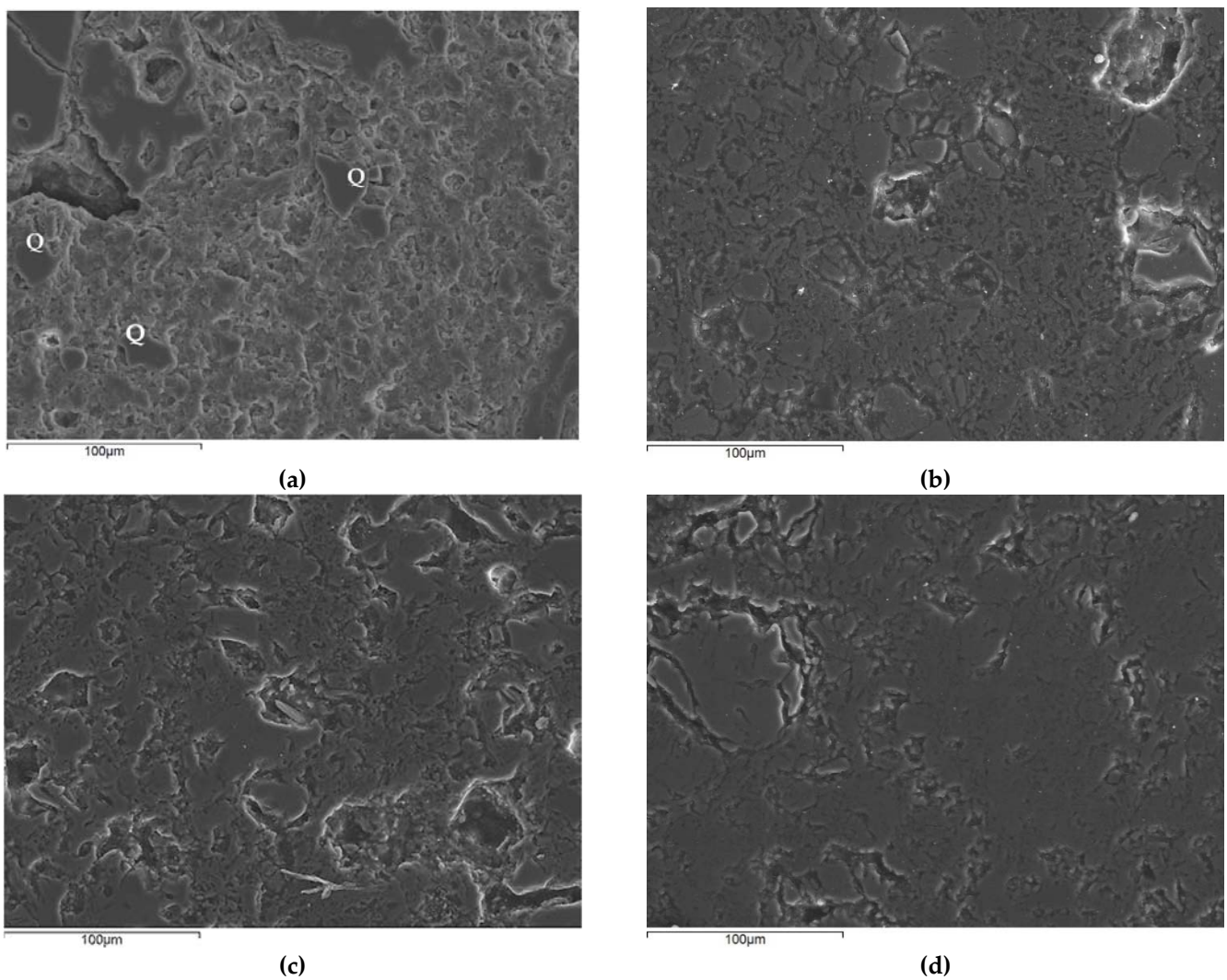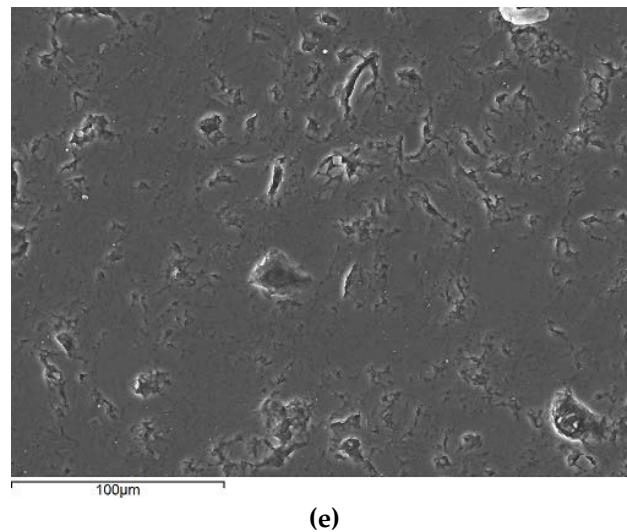

Figure 7. *Cont.*

(e)

Figure 7. Secondary electrons' images of polished surfaces of (**a**) the reference clay-body, (**b**) W20, (**c**) W50, (**d**) W80, and (**e**) CSM, fired at 1000 °C. Scale is 100 μm. Magnification (×400).

4. Conclusions

This preliminary study investigated the potential valorization of a high-smectite clayey sterile material from the Prosilio region (Kozani, NW Greece) in the application field of traditional ceramics, e.g., roofing tiles and/or bricks. The samples manufactured at lab-scale were evaluated in terms of physical and mechanical properties, as well as for their crystalline phases formation and microstructural evolution after firing at 1000 °C. From the obtained results, it can be concluded that CSM should be considered as a viable substitute for a calcium-rich clay-body, since additions up to 50 wt% resulted in end products with technological properties comparable to the reference clay-body. The increase in CSM to 80 wt% led to the reduction in porosity and water absorption values, whereas bulk density and linear shrinkage increased both, but with no coherent increase in bending strength. For the latter formulation, increased iron oxide content in CSM in conjunction with the lower mineralizer oxides (CaO) and fillers (quartz) led to the formation of a weak crystalline structure and an enhanced liquid phase upon firing.

However, for the manufacturing of qualitative ceramic end products, the above-stated issues can be regulated starting from the design of the batches with respect to the raw material's chemical and mineralogical composition. Under this prism, clayey sterile materials, along with other characteristics (e.g., lower smectite contents), could improve the sintering behavior of the tested samples due to the contained clay minerals.

Conflicts of Interest: The authors declare no conflict of interest.

References

1. Mining Waste: A Potential Ceramic Resource—European Training Network for the Remediation and Reprocessing of Sulfidic Mining Waste Sites. Available online: https://etn-sultan.eu/2021/02/25/mining-waste-a-potential-ceramic-resource/ (accessed on 9 June 2021).
2. Romero, M.; Padilla, I.; Contreras, M.; López-Delgado, A.; Kalinkin, M. Minerals Mullite-Based Ceramics from Mining Waste: A Review. *Minerals* **2021**, *11*, 332. [CrossRef]
3. Aznar-Sánchez, J.A.; García-Gómez, J.J.; Velasco-Muñoz, J.F.; Carretero-Gómez, A. Mining waste and its sustainable management: Advances in worldwide research. *Minerals* **2018**, *8*, 284. [CrossRef]
4. Popovic, V.; Miljkovic, J.Ž.; Subic, J.; Jean-Vasile, A.; Adrian, N.; Nicolaescu, E. Sustainable land management in mining areas in Serbia and Romania. *Sustainability* **2015**, *7*, 11857–11877. [CrossRef]
5. Perez-Santana, S.; Pomares Alfonso, M.; Villanueva Tagle, M.; Peña Icart, M.; Brunori, C.; Morabito, R. Total and partial digestion of sediments for the evaluation of trace element environmental pollution. *Chemosphere* **2007**, *66*, 1545–1553. [CrossRef] [PubMed]
6. EUR-Lex—32006L0021—EN—EUR-Lex. Available online: https://eur-lex.europa.eu/legal-content/EN/TXT/?uri=CELEX%3A3 2006L0021 (accessed on 9 June 2021).
7. The Paris Agreement | UNFCCC. Available online: https://unfccc.int/process-and-meetings/the-paris-agreement/the-paris-agreement (accessed on 10 June 2021).
8. EUR-Lex—52019DC0640—EN—EUR-Lex. Available online: https://eur-lex.europa.eu/legal-content/EN/TXT/?qid=158858 0774040&uri=CELEX:52019DC0640 (accessed on 9 June 2021).
9. Durucan, S.; Korre, A.; Munoz-Melendez, G. Mining life cycle modelling: A cradle-to-gate approach to environmental management in the minerals industry. *J. Clean. Prod.* **2006**, *14*, 1057–1070. [CrossRef]
10. Laurence, D. Establishing a sustainable mining operation: An overview. *J. Clean. Prod.* **2011**, *19*, 278–284. [CrossRef]
11. Rodrigues, R.; Santana, L.N.L.; Arajo, G.; Carlos, H. *Recycling of Mine Wastes as Ceramic Raw Materials: An Alternative to Avoid Environmental Contamination*; Srivastava, J., Ed.; InTech: Rijeka, Croatia, 2012; ISBN 978-953-51-0120-8.
12. Loutou, M.; Taha, Y.; Benzaazoua, M.; Daafi, Y.; Hakkou, R. Valorization of clay by-product from moroccan phosphate mines for the production of fired bricks. *J. Clean. Prod.* **2019**, *229*, 169–179. [CrossRef]
13. Contreras, M.; Gázquez, M.J.; Romero, M.; Bolívar, J.P. 5—Recycling of industrial wastes for value-added applications in clay-based ceramic products: A global review (2015–19). In *New Materials in Civil Engineering*; Samui, P., Kim, D., Iyer, N.R., Chaudhary, S., Eds.; Butterworth-Heinemann: Oxford, UK, 2020; pp. 155–219. ISBN 978-0-12-818961-0.
14. Petrounias, P.; Rogkala, A.; Giannakopoulou, P.P.; Lampropoulou, P.; Koutsovitis, P.; Koukouzas, N.; Laskaris, N.; Pomonis, P.; Hatzipanagiotou, K. Removal of Cu (II) from industrial wastewater using mechanically activated serpentinite. *Energies* **2020**, *13*, 2228. [CrossRef]
15. INVALOR—Research Infrastructure for Waste Valorization and Sustainable Management of Resources. Available online: https://www.invalor.org/ (accessed on 20 August 2021).
16. Global Ceramics Market Size | Industry Analysis Report. 2019. Available online: https://www.grandviewresearch.com/industry-analysis/ceramics-market (accessed on 9 June 2021).
17. *Global Resources Outlook 2019: Natural Resources for the Future We Want*; A Report of the International Resource Panel (IRP); United Nations Environment Programme (UNEP): Nairobi, Kenya, 2019.
18. Eurostat. Waste Statistics—Statistics Explained. Available online: https://ec.europa.eu/eurostat/statistics-explained/index.php?title=Waste_statistics#Total_waste_generation (accessed on 15 June 2021).
19. Dondi, M.; Iglesias, C.; Dominguez, E.; Guarini, G.; Raimondo, M. The effect of kaolin properties on their behaviour in ceramic processing as illustrated by a range of kaolins from the Santa Cruz and Chubut Provinces, Patagonia (Argentina). *Appl. Clay Sci.* **2008**, *40*, 143–158. [CrossRef]
20. Starý, J.; Jirásek, J.; Pticen, F.; Zahradník, J.; Sivek, M. Review of production, reserves, and processing of clays (including bentonite) in the Czech Republic. *Appl. Clay Sci.* **2021**, *205*, 106049. [CrossRef]
21. Zaidan, S.A.; Abdull-Razzak, S.S. Effect of bentonite addition on some properties of porcelain. *J. Eng.* **2018**, *25*, 84–99. [CrossRef]
22. Christogerou, A.; Kavas, T.; Pontikes, Y.; Rathossi, C.; Angelopoulos, G.N. Evolution of microstructure, mineralogy and properties during firing of clay-based ceramics with borates. *Ceram. Int.* **2010**, *36*, 567–575. [CrossRef]
23. Gutiérrez Bayona, A.; Obando Gamboa, C.J.; Moreno Moreno, C.J. Caracterización físico-mecánica del estéril de carbón, en busca de una alternativa ambiental para las obras de infraestructura civil. *Investig. Innovación Ing.* **2018**, *6*, 16–29. [CrossRef]
24. Amrani, M.; Taha, Y.; El Haloui, Y.; Benzaazoua, M.; Hakkou, R. Sustainable reuse of coal mine waste: Experimental and economic assessments for embankments and pavement layer applications in morocco. *Minerals* **2020**, *10*, 851. [CrossRef]
25. Stolboushkin, A.Y.; Ivanov, A.I.; Fomina, O.A. Use of Coal-Mining and Processing Wastes in Production of Bricks and Fuel for Their Burning. *Procedia Eng.* **2016**, *150*, 1496–1502. [CrossRef]
26. Žibret, G.; Lemiere, B.; Mendez, A.M.; Cormio, C.; Sinnett, D.; Cleall, P.; Szabo, K.; Carvalho, T. National mineral waste databases as an information source for assessing material recovery potential from mine waste, tailings and metallurgical waste. *Minerals* **2020**, *10*, 446. [CrossRef]

27. Zurita Ares, M.C.; Pérez, M.R.; Quesada Carballo, L.; Fernández, J.M. Assessment of clays from Puertollano (Spain) for their use in fine ceramic by diffuse reflectance spectroscopy. *Appl. Clay Sci.* **2015**, *108*, 135–143. [CrossRef]

28. Doutsos, T.; Pe-Piper, G.; Boronkay, K.; Koukouvelas, I. Kinematics of the central Hellenides. *Tectonics* **1993**, *12*, 936–953. [CrossRef]

29. Doutsos, T.; Koukouvelas, I. Fractal analysis of normal faults in northwestern Aegean area, Greece. *J. Geodyn.* **1998**, *26*, 197–216. [CrossRef]

30. Koukouvelas, I. *The Geology of Greece*, 1st ed.; LIBERAL BOOKS: Athens, Greece, 2018; ISBN 9786185012403. (In Greek)

31. Bender, W.; Händle, F. (Eds.) *Brick and Tile Making. Procedures and Operating Practice in the Heavy Clay Industries*; Bauverlag GmbH: Wiesbaden/Berlin, Germany, 1982; ISBN 3-7625-1485-2.

32. ASTM C326-82(1997)e1. *Standard Test Method for Drying and Firing Shrinkages of Ceramic Whiteware Clays*; ASTM International: West Conshohocken, PA, USA, 1997.

33. ASTM C373-88(2006). *Standard Test Method for Water Absorption, Bulk Density, Ap-parent Porosity, and Apparent Specific Gravity of Fired Whiteware Products*; ASTM International: West Conshohocken, PA, USA, 2006.

34. Christogerou, A.; Kavas, T.; Pontikes, Y.; Koyas, S.; Tabak, Y.; Angelopoulos, G.N. Use of boron wastes in the production of heavy clay ceramics. *Ceram. Int.* **2009**, *35*, 447–452. [CrossRef]

35. Mackenzie, R.C.; Bishui, B.M. The Montmorillonite Differential Thermal Curve. ii Effect of Exchangeable Cations on the Dehydroxylation of Normal Montmorillonite. *Clay Miner. Bull.* **1958**, *3*, 276–286. [CrossRef]

36. Smykatz-Kloss, W.; Heide, K.; Klinke, W. Chapter 11: Applications of thermal methods in the geosciences. In *Handbook of Thermal Analysis and Calorimetry*; Elsevier: Amsterdam, The Netherlands, 2003; Volume 2, pp. 451–593. ISBN 9780444820860.

37. Mackenzie, R.C. Simple Phyllosilicates Based on Gibbsite- and Brucite-like Sheets. *Differ. Therm. Anal.* **1971**, *1*, 775.

38. Taylor, R.K.; Smith, T.J. The engineering geology of clay minerals: Swelling, shrinking and mudrock breakdown. *Clay Miner.* **1986**, *21*, 235–260. [CrossRef]